SEISMIC RISK ASSESSMENT OF ITALIAN SEAPORTS: THE CASE OF ANCONA (ITALY)

V. Pessina[1], L. Scandella[1], G. Franceschina[1], C.G. Lai[2]

[1] *Istituto Nazionale di Geofisica e Vulcanologia (INGV), Milano, Italy*
[2] *European Centre for Training and Research in Earthquake Engineering (EUCENTRE), Pavia, Italy*
Email:pessina@mi.ingv.it

ABSTRACT :

A National research project was recently carried out to develop a robust methodology for the design and retrofit of wharves structures located in areas of high to moderate seismicity. A detailed census of the Italian major seaports was performed using purposely devised questionnaires and Ancona harbor was chosen for a detailed investigation with the aim of providing risk assessment guidelines. This port has been selected as representative of a moderate seismicity area (expected peak ground acceleration of 0.25 g with a return period of 475 yrs). Ancona is the first harbor in the Adriatic sea, with more than a 1.500.000 passenger service and 150.000 trucks transit. It is equipped with 30 wharfs, 25 of which built in 1965-1975.
To compute deterministic ground shaking scenarios, predictive empirical models have been used. At the same time advanced numerical simulation have been carried out both at high (0.7-30 Hz) and low (0-1.3) frequency ranges. The contributions of site effects and liquefaction have been also taken into account in damage estimation. Standard risk assessment has been performed using the empirical curves implemented in HAZUS program (NIBS, 2004), supported by recent studies (Lessloss, 2006, Del. 89) on damage observed after the 2003 event in Lefkas (Greece).

KEYWORDS: deterministic ground shaking scenario, numerical simulations, seaport damage, risk assessment

1   INTRODUCTION

The poor performance exhibited by seaports structures in recent earthquakes (e.g. 1989 Loma Prieta in US, 1995 Hyogoken-Nambu and 2003 Tokachi-Oki in Japan, Lefkas in Greece, 1999) has spurred an intense research activity worldwide to set up methodologies and technical recommendations (see for instance the guidelines issued by the International Navigation Association, 2001) for a proper seismic design of new port structures and an appropriate retrofitting of existing ones improving their expected performance in case of seismic events.
In Italy, following this general trend, a research project has been funded by the Italian Department of Civil Protection with the aim to: 1) develop a robust methodology for the design of marginal wharves structures located in zones from high to moderate seismicity and 2) define the interventions of seismic retrofitting of existing marginal wharves to reduce their seismic vulnerability for the expected ultimate limit state design earthquake. Within this project a detailed census of the Italian major seaports was carried out using purposely devised and calibrated questionnaires. The items inserted in the questionnaires concerned with the most relevant structural and geotechnical features affecting the seismic vulnerability of wharf structures together with some indicators defining the strategic role played by the port at the national level. Among the seaports selected for the census, Ancona in Central Italy has been chosen as the case study to show the adopted methodology for deterministic hazard and damage assessment of seaports. It is located in a moderate seismic zone (http://esse1-gis.mi.ingv.it/), with a well documented seismic history (http://emidius.mi.ingv.it/DBMI04/).

2   GROUND SHAKING SCENARIOS

Deterministic ground shaking scenarios have been computed as the first step of a risk analysis: to this aim both

predictive empirical models and advanced numerical simulation have been carried out.

Two faults, identified by the Italian Database of Individual Seismogenic Sources (DISS v.3.0.4, 2007, http://legacy.ingv.it/DISS) have been adopted as seismic sources. In particular, the Senigallia (ITGG030) and the Conero-Offshore (ITGG029) ones are of interest for the Ancona seaport (Figure 1), both with a potential M5.9 and an approximate distance from the city of about 12 km. The Senigallia fault, the best defined and constrained, is considered responsible of the 1930 event (MCS Intensity=VIII in Ancona) (Basili et al., 2007) and it has been assumed as the reference source for the produced scenarios, herein presented.

Ground motion parameters have been evaluated in high (0.7-30 Hz) and low (0-1.3) frequency ranges, using the Deterministic-Stochastic Method (DSM) of Pacor et al. (2005) and the semi-analytical approach of Hisada & Bielak (2003), respectively.

Site effects have been taken into account applying proper coefficients to the ground motion values predicted by empirical relationships or performing 1D analytical analyses by the EERA code (Equivalent-linear Earthquake site Response Analysis, 2000, http://gees.usc.edu/GEES/Software/EERA2000/Default.htm.).

2.1 *Empirical predictions*

As no recording data are available to calibrate numerical simulations, the comparison between advanced simulations and empirical estimations suggests the choice of the scenario closer to the medium empirical trend. On the other hand, advanced simulations provide a ground shaking including physical effects that can be scarcely reproduced by attenuation relationships only.

Adopting the most recent attenuation relationships the comparisons in terms of peak values have been done with the empirical values illustrated in Table 1, calculated in Ancona for the case of ITGG030 fault.

Table 1 Empirical peak ground motion on rock condition in Ancona (M5.9 and distance 13.9 km)

Parameter	Empirical estimation (mean value)	Attenuation relationship
PGA [g]	0.143	AMB05 (Ambraseys et al., 2005a) max horizontal component
	0.162	AMB03 (Ambraseys et al., 2003) max horiz. comp., near field (< 15 km)
	0.116	SP96 (Sabetta and Pugliese, 1996) max horizontal component
	0.124	TB02 (Tromans and Bommer , 2002) max horizontal component
	0.069	AMB05 (Ambraseys et al., 2005b) vertical component
	0.088	AMB03 vertical component, near field
	0.056	SP96 vertical component
PGV [cm/s]	8.34	AMB07 (Akkar & Bomber, 2007) max horizontal component
	6.97	AMB07 mean horizontal component
	6.56	SP96 max horizontal component
	3.71	SP96 vertical component
	7.14	TB02 max horizontal component
PGD [cm]	1.4 - 2.2	FC08 (Cauzzi and Faccioli, 2008) max horizontal component
	1.1	TB02 max horizontal component

2.2 *Numerical results for rock conditions*

Bedrock seismic response has been evaluated performing 3D numerical analyses of the seismic source and of the propagation path in a layered configuration. The high frequency DSM allows the generation of ground motion due to an extended fault using the isochron theory (Bernard & Madariaga, 1984; Spudich & Frazer, 1984) to generalize the point source stochastic method of Boore (2003). The low frequency Hisada method simulates the complete 3D wave propagation field induced by an extended kinematic source based on the static and dynamic Green functions, allowing the evaluation of the permanent ground displacement. Both the methods are proper to simulate the seismic ground response in near fault rupture conditions and to reproduce directivity effects. Parametric analyses have been performed varying the hypocentre location on the fault to analyse the potential directivity effects towards the harbor. As shown in Figure 1, 10 locations (P_i and M_i i=1,5) of the hypocentre have been assumed in the deeper portion of the fault.

Fault parameters adopted for both high and low frequency simulations of the ITG030 source are reported in Figure 1, where the assumed 1D crustal model is also shown (see EUCENTRE-PE5, 2008, for details). A homogeneous slip distribution and a constant rupture velocity of 2.6 km/s were employed. Moreover, both Hisada method and DSM require specific simulation parameters like the rise time (T_r = 0.8 s) and a depth dependent quality factor ($Q_L = Q_L^0 f$) for Hisada, or a spectral attenuation model (specified in terms of quality factor $Q(f) = 35 \cdot f$ in accordance with Del Pezzo et al.,1985, and high frequency spectral decay, k = 0.024 s) for DSM.
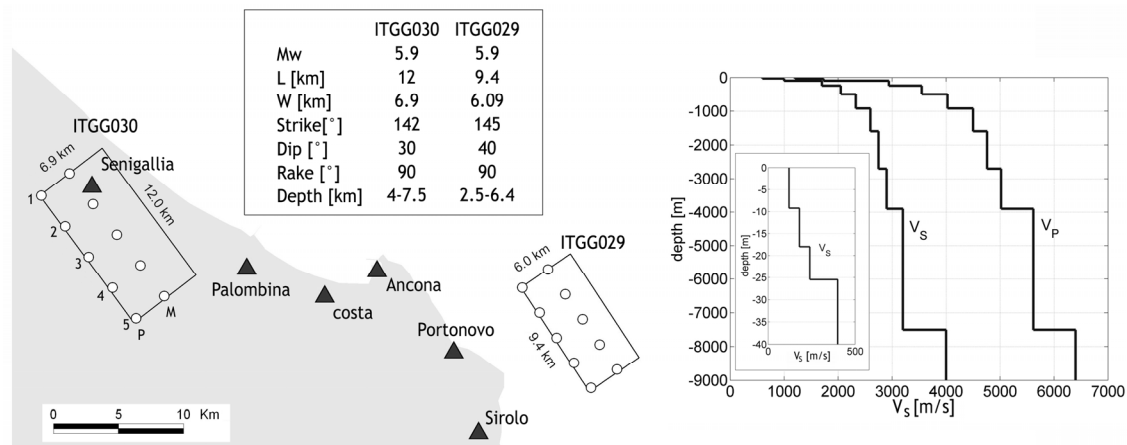

Figure 1 Hypocentres location on the Senigallia (ITGG030, West) and Conero-Offshore (ITGG029, East) faults. Location of the six receivers adopted for simulations are also shown (full triangles). The insets on the right and on the left refer to the assumed fault parameters and 1D crustal model, respectively.

The ground velocity is the best parameter of comparison between the seismic responses evaluated by the two numerical approaches. The PGV values due to the activation of the assumed hypocenters are listed in Table 2; in particular the mean values between the horizontal components simulated in Ancona are reported.

As a consequence of the extended fault and directivity effects , the variability of the ground shaking depends on both the distance and the position of the site respect to the source.

In Ancona PGV between 1.1 and 10.8 cm/s have been estimated in the high frequency range with the maximum due to M2, while values between 1.4 and 7.4 cm/s have been evaluated by low frequency simulations, with a maximum due to P3. The DSM gives a higher amplification which is in reasonable agreement with the empirical estimations as shown in Figure 2a. In particular hypocentres M3, M1 and P2 gives the PGV values in best agreement with the empirical mean values. This result is also confirmed in terms of pseudo velocity spectra (Figure 2b) and acceleration spectra (Figure 2c).

It turns out that, the most critical rupture models (P1, M1, P2, M2) generate a ground shaking in agreement with the medium value predicted by the empirical spectral relations. Otherwise, one can alternatively say that the use of empirical attenuation relations allows to produce scenarios representing the worst possible cases of nucleation for this particular combination of magnitude and distance.

Table 2 Seismic ground parameters estimated in Ancona for the activation of 10 hypocentres

	P1	P2	P3	P4	P5	M1	M2	M3	M4	M5
DSM PGA [g]	0.178	0.184	0.0825	0.0397	0.0214	0.162	0.220	0.121	0.0428	0.0142
DSM PGV [cm/s]	9.97	9.32	5.10	2.88	1.70	8.63	10.80	5.92	2.77	1.11
Hisada PGV [cm/s]	5.14	6.57	7.39	5.19	1.53	4.65	5.01	5.53	5.37	1.42

2.3 *Site effects and liquefaction*

To consider local soil conditions using empirical relations, multiplicative coefficients have been applied for the soil class "soft" ($180 < V_{S30} < 360$ m/s) and "very soft" ($V_{S30} < 180$ m/s assumed for harbour fillings). Site effects have been also estimated by 1D analytical analyses using as input excitation the acceleration seismic response evaluated by the DSM bedrock simulations, that have been considered sufficiently representative

concerning the frequency content, as shown by the spectra values of Figure 2. The low frequency results, necessary for the estimation of permanent displacement (equals to about 1-1.6 mm), have not been used at this stage, since not significant in terms of acceleration. Both linear and viscoelastic linear–equivalent behaviours have been investigated. As expected, the amplification peaks decrease in linear-equivalent case and shift to low frequencies. Neglecting non-linearity, soil amplification is overestimated, with a factor up to 3 in Ancona. While the numerical linear-equivalent analyses amplify less than the empirical ones, the contrary happens in linear field (Figure 3): the mean acceleration evaluated by DSM of 0.1 g is amplified up to 0.19 g and 0.12 g in linear and linear-equivalent behaviour respectively.

Among the numerous approaches to evaluate the liquefaction potential (Lessloss, Del. 87, 2006), the method of Juang et al. (2003) has been applied for its simplicity and replicability. Using M5.9 and PGA of 2.084 m/s^2, equals to the maximum value calculated on rock by DSM due to nucleation P1, a low probability of liquefaction is expected; in fact a value of $P_L > 45\%$ ($F_S < 1$) has been observed at 6 m depth just in one thin layer. Successively, using the Zhang et al. (2002) method, a settlement of about 8.8 cm has been estimated.
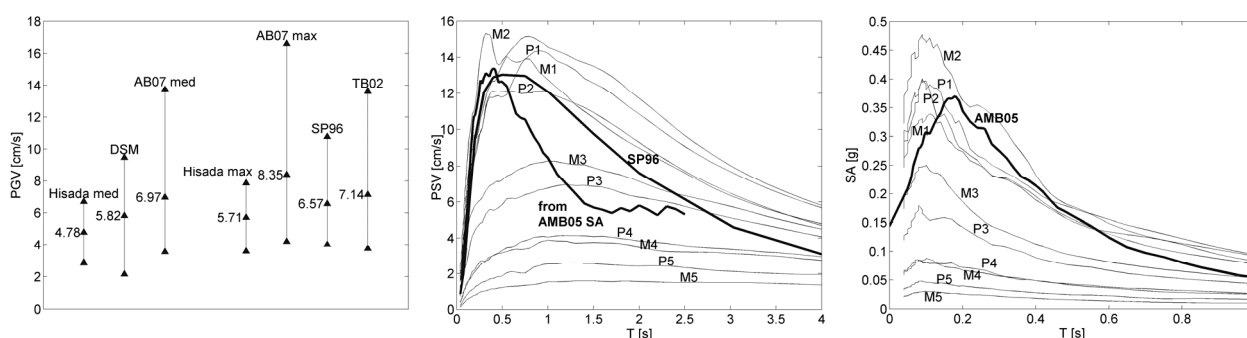

Figure 2 Comparison among PGV values (m, m ± s.d.) evaluated by DSM, Hisada method and empirical models AB07 (mean and maximum horizontal values), SP96 and TB02 (maximum values) (left); pseudo velocity spectra PSV obtained by DSM (thin lines), SP96 and AMB05 (from SA) (centre); acceleration spectra SA by DSM (thin lines) and AMB05 (bold line) (right)
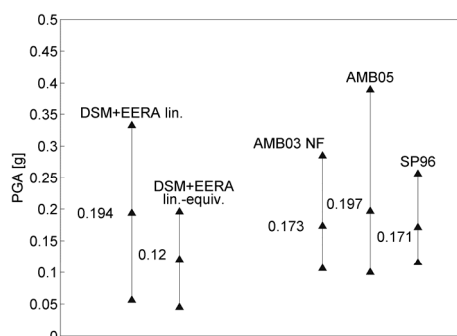

Figure 3 Comparison between PGA values (mean horizontal component) obtained by 1D linear and linear-equivalent analyses with empirical predictions

3   DAMAGE ASSESSMENT OF SEAPORTS

Harbours represent complex systems of elements with different features and vulnerability. Port facilities can be classified in three main categories:
  a)   waterfront structures: wharves (port embankments), seawalls (protective caisson walls from erosion) and piers (break-water structures which form harbours). These structures typically are supported by wood, steel or concrete piles and in many cases batter piles.
  b)   Cranes, cargo handling and storage equipment: stationary or rail mounted (anchored/unanchored) structures used to load and unload vessels, tanks.

c) Port infrastructures:
   i. transportation systems: railway, roadway;
   ii. buildings: structures used as traffic control, passenger terminals, offices, maintenance, sheds and warehouses;
   iii. utility systems: electric power, communication, potable water, waste water, fuel facilities (fuel storage tanks, pump equipment, piping, backup power systems).

Methods for damage assessment of harbour systems have been collate during the recent European projects Risk_Ue (Monge et al., 2004), (Pitilakis et al., 2006) and Lessloss (Del. 87, 2006), after the relevant observed damage caused by the severe events in Greece (2003) and Turkey (1999). Although damage assessment procedures are based on American and Japanese data, a recent study for Lefkas seaport (Kakderi et al., 2006) has shown that these methods can be reasonably used in European context also, where few damage data are available. Following HAZUS procedure, damage to harbour components is classified in five levels: slight/minor, moderate, extensive, complete. Damage to each component is estimated by vulnerability curves defined as (cumulative) lognormal distribution functions, giving the probability of reaching or exceeding different levels of damage as a function of ground motion.

Vulnerability curves for each component uses different ground motion parameters. In particular, for the previous described categories, curves are defined as function of:
   a) permanent ground displacement (perm_GD);
   b) peak ground acceleration (PGA) and permanent ground displacement (perm_GD) ;
   c) i. railway: permanent ground displacement (perm_GD);
      ii. depending on damage assessment methods proper for buildings;
      iii. function of the utility component: PGA and perm_GD for fuel facilities; PGV or strain (PGS) for buried pipelines, or proper curves (NIBS 2004; Monge et al., 2004; Pitiliakis et al., 2006; ALA, 2001).

Kakderi et al. (2006), performing the vulnerability and damage assessment for Lefkas seaport (Greece), concluded that the damage state distribution based on HAZUS relationships is rather compatible with the observed one for quay walls, while Ichii (2003) curves, based on finite elements analysis, seems to gives overestimated results. Moreover, the latter functions require the knowledge of geotechnical and construction data, not always available, but they are useful when the permanent ground displacement required in HAZUS is not evaluated.

3.1 The case of Ancona

The Ancona harbour (Figure 4) is equipped by various piers (7) and wharves (25) with different structural typology (piles, sheet pilings, rock pylons and gravity-type walls), different use destination and type of traffic. While no distinction has been done between waterfront components in assessing damage, cargo equipment has been classified between anchored and unanchored. Information on fuel facilities and hydraulic system are not available.
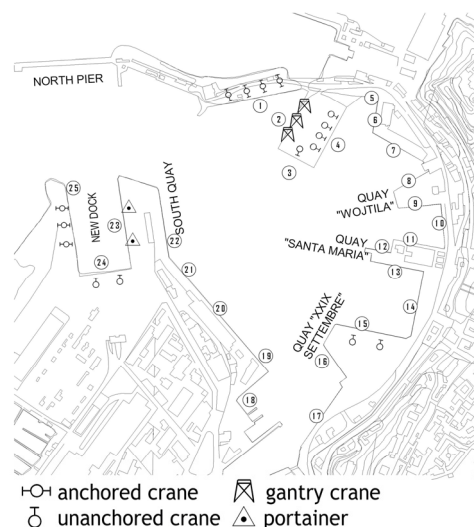

Figure 4 Location of the harbour components analysed in damage assessment

Damage due to wave propagation has been estimated including site effects for linear-equivalent behaviour. Results are shown for the P2 hypocentre, which represents one of the most critical scenarios in Ancona. It turns out that, unanchored structures (cargo and fuel facilities) are more vulnerable than the anchored ones. The probability of exceeding the slight damage is higher than 60% and 90% for cargo and fuel facilities respectively, the exceeding probability of moderate damage is higher than 15% and 50% respectively. In case of linear behaviour analyses, the damage probability increases up to 40-50%.

A significant static contribution due to liquefaction is estimated equals to about 8.8 cm but, being low the probability of liquefaction (0.23 %), waterfront structures (category a) and railway tracks (category c-i) are expected to not be damaged.

It is important to highlight that, when both dynamic (wave propagation) and permanent effects (as fault rupture, settlements and lateral spreading due to liquefaction) have the probability to damage a harbour structure, the total probability to exceed a damage level must be evaluated combining the partial contributes.

The unanchored cargo/storage equipment (category b) and the unanchored fuel facilities (category c-iii) are the harbour components with relevant probability of damage; the occurrence percentages of their damage levels and the percentages of the serviceability are listed in Table 3. Following Pachakis e Kiremidjian (2004) the loss of serviceability has been estimated as the probability to reach at least the moderate level of damage (sum of percentages of moderate, extensive and total levels).

As a consequence, according to HAZUS methodology, the time required for the serviceability restoration is less than 1 day for unanchored cargo and storage equipment and less than 2 days for fuel facilities (related to 55% of probability of no serviceability), as shown in Figure 6.
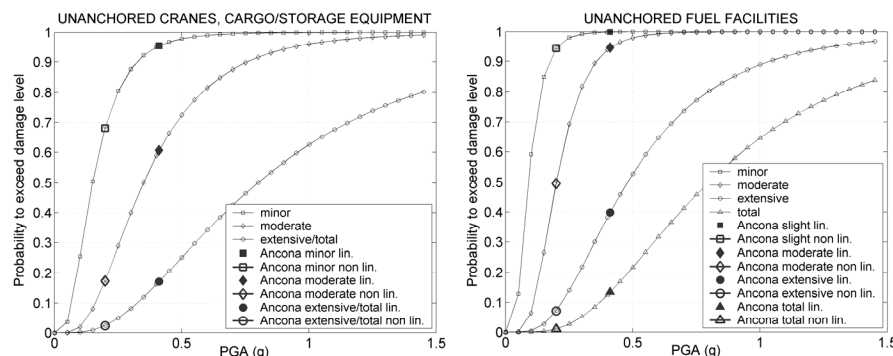

Figure 5 Vulnerability curves for rail mounted cranes and cargo/storage equipment (left) and unanchored fuel facilities (right). Damage probabilities due to P2 nucleation are overlapped: results estimated in linear (solid symbols) and non-linear (open symbols) field.

Table 3 Damage probability and serviceability of unanchored cranes, cargo/storage equipment (category b) and fuel facilities (category c-iii)

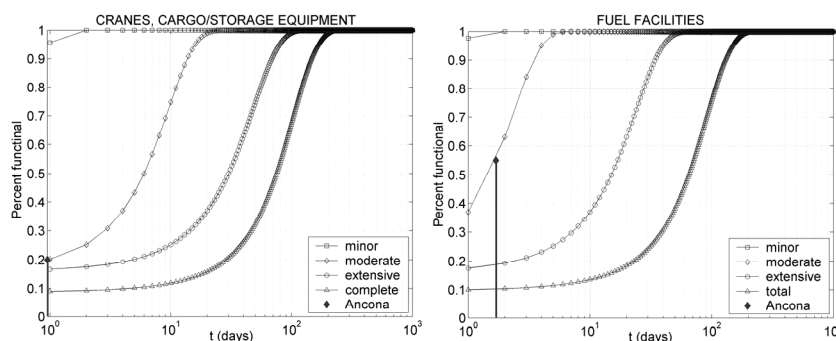| UNANCHORED CRANES, CARGO/STORAGE EQUIPMENT		
Null	28 %	80 % serviceability
Slight/Minor	52 %	
Moderate	13 %	20 % serviceability
Extensive/Total	3 %	
UNANCHORED FUEL FACILITIES		
Null	4 %	45 % serviceability
Slight/Minor	41 %	
Moderate	46 %	55 % serviceability
Extensive	8 %	
Total	1 %	

Figure 6 Restoration curves and expected time for serviceability restoration of the most damaged structures in the Ancona harbor: cargo/storage equipment (left), fuel facilities (right)

4   CONCLUSIONS

Damage to seaport structures in recent earthquakes has promoted an intense research activity. Recent analyses have been carried out in Europe, in particular in Greece after the Lefkas event, while in Italy there are no evidence of particular case-studies or methodology for harbour damage assessments. The aim of this contribution is to outline a standard procedure for harbours damage assessment in Italian seismic zones. The proposed method, has been calibrated on the case of Ancona. To this aim, different deterministic hazard scenarios have been generated to ponder the variability of the seismic response into the damage assessment. Beside the generation of empirical ground shaking scenarios, two different numerical methods have been employed to simulate low (0-1.3) and high (0.7-30 Hz) frequency range scenarios, respectively. Both methods are able to evaluate the influence of finite fault and directivity effects. Site amplification and liquefaction have been also taken into account by 1D linear-equivalent analyses.

Since the lack of European data, damage probability to harbor structures has been estimated using HAZUS (NIBS, 2004) procedure, after its recent validation (Lessloss, 2006, Del.89).

REFERENCES

Akkar S., Bommer J.J. (2007). Empirical prediction equations for peak ground velocity derived da strong-motion records da Europe and the Middle East. *Bull. Seism. Soc. Am.* **97:2**, 511-530.

Ambraseys N. N., Douglas J., Sarma S. K., Smit P. M. (2005a). Equations for the estimation of strong ground motions da shallow crustal earthquakes using data da Europe and the Middle East: horizontal peak ground acceleration and spectral acceleration. *Bull. Earthquake Eng.* **3:1**, 1-53.

Ambraseys N. N., Douglas J., Sarma S. K., Smit P. M. (2005b). Equations for the estimation of strong ground motions da shallow crustal earthquakes using data da Europe and the Middle East: vertical peak ground acceleration and spectral acceleration. *Bull. Earthquake Eng.* **3:1**, 55-73.

Ambraseys N.N. & Douglas J. (2003). Near-field horizontal and vertical earthquake ground motions. *Soil Dynamics and Earthquake Engineering* **23:1**, 1-18.

Basili R., Burrato P., Mariano S., Mirabella F., Ravaglia A., Valensise G., Vannoli P. (2007). Identification and

characterization of seismogenetic sources for seismic hazard scenarios along the Marche coastline (in Italian). Mucciarelli M.,Tiberi P. (eds.), Tecnoprint srl Ancona, 3-70.

Bernard P., Madariaga R. (1984). A new asymptotic method for the modeling of near field accelerograms. *Bull. Seismol. Soc. Am.* **74:2**, 539-557.

Boore D.M. (2003). Simulation of ground motion using the stochastic method, *Pure Appl. Geophys*. **160**, 635-676.

Cauzzi C., Faccioli, E. (2008). Broadband (0.05 a 20 s) prediction of displacement response spectra based on worldwide digital records. *J Seismol.* **3**, DOI 10.1007/s10950-008-9098-y.

Del Pezzo E., Rovelli A., Zonno G. (1985). Seismic Q and site effects on seismograms of local earthquakes in the Ancona region (central Italy). *Annales Geophysicae* **3:5**, 629-636.

EUCENTRE-PE5 (2008). Progettazione Sismica di Strutture Portuali Marittime. *Research Report*, European Centre for Training and Research in Earthquake Engineering. July 2008, pp. 201 (in Italian).

Hisada Y., Bielak J. (2003). A theoretical method for computing near fault ground motion in a layered half-spaces considering static offset due to surface faulting, with a physical interpretation of fling step and rupture directivity. *Bull. Seismol. Soc. Am.* **93:3**, 1154-1168.

Ichii K. (2004). Fragility curves for gravity-type quay walls based on effective stress analysis. *Proc. 13th WCEE*, Vancouver, BC Canada.

Juang C.H., Yuan H., Lee D.H., Lin P.S. (2003). Simplified Cone Penetration Test-based method for Evaluating Liquefaction Resistance of Soils. *Journal of Geotechnical and Geoenvironmental Eng.* ASCE **129:1**, 66-80.

Kakderi K., Raptakis D., Argyroudis S., Alexoudi M., Pitilakis K. (2006). Seismic Response and Vulnerability Assessment of Quaywalls. The Case of Lefkas. *Proceedings of the 5th National Conference of Geotechnical and Environmental Engineering*, Xanthi, Greece (in Greek).

Lessloss (2006). Deliverable 89 - Technical report on the assessment of vulnerability functions for pipelines, shallow tunnels and waterfront structures. Sub-Project 11 – Earthquake disaster scenario predictions and loss modelling for infrastructures. Lessloss Project - Risk mitigation for earthquake and landslides integrated project - Project No.: GOCE-CT-2003-505488.

Monge O., Alexoudi M., Argyroudis S., Martin C., Pitilakis K. (2004). Vulnerability assessment of lifelines and essential facilities (WP06): basic methodological handbook. Risk_UE An advanced approach to earthquake risk scenarios with application to different european towns, Research Project, European commission, DG XII2001-2004, CEC Contract number EVK4-CT-2000-00014.

NIBS (National Institute of Building Sciences) (2004). Earthquake loss estimation methodology, HAZUS. Thecnical manual, Federal Emergency Management Agency, Washington, D.C.

Pachakis D. & Kiremidjian A.S. (2004). Estimation of Downtime-related revenue losses in seaport following scenario earthquakes. *Earthquake Spectra* **20:2**, 427-449.

Pacor, F., Cultrera, G., Mendez, A. , Cocco, M. (2005). Finite Fault Modeling of Strong Ground Motion Using a Hybrid Deterministic - Stochastic Method. *Bull. Seismol. Soc. Am.* **95:1**, 225-240.

Pitilakis K., Alexoudi A., Argyroudis S., Monge O., and Martin C. (2006). Chapter 9: Vulnerability assessment of lifelines. in C.S. Oliveira, A. Roca and X. Goula ed. "Assessing and Managing Earthquake Risk. Geo-Scientific and Engineering Knowledge for Earthquake Risk mitigation: Developments, Aols and Techniques," Springer Publ.

Roth W.H., & Dawson E.M. (2003). Analysing the seismic performance of wharves, part 2: SSI analysis with non-linear, effective-stress soil models. *Proceedings of the 6th U.S. Conference and Workshop of lifeline Earthquake Engineering TCLEE*, Monograph No. **25**, August.

Sabetta F. & Pugliese A. (1996). Estimation of response spectra and simulation of nonstationary earthquake ground motion. *Bull. Seism. Soc. Am.* **86:2**, 337–352.

Spudich P., Frazer N.L. (1984). Use of ray theory to calculate high-frequency radiation from earthquake sources having spatially variable rupture velocity and stress drop. *Bull. Seismol. Soc. Am.,* **74:6,** 2061-2082.

Tromans I.J., Bommer J.J. (2002). The attenuation of strong-motion peaks in Europe. *Proceedings of the Twelfth European Conference on Earthquake Engineering, London*, Monograph No. **394**.

Zhang G., Robertson P.K., Brachman R. W. I. (2002). Estimating liquefaction-induced ground settlements from CPT for level ground. *Can. Geotech. J.* **39**, 1168-1180, DOI: 10.1139/T02-047.